HHS Public Access

Author manuscript

Nat Med. Author manuscript; available in PMC 2010 July 27.

Published in final edited form as:

Nat Med. 2009 March ; 15(3): 325–330. doi:10.1038/nm.1916.

Hypernitrosylated ryanodine receptor/calcium release channels are leaky in dystrophic muscle

Andrew M. Bellinger[1], **Steven Reiken**[1], **Christian Carlson**[1], **Marco Mongillo**[1], **Xiaoping Liu**[1], **Lisa Rothman**[1], **Stefan Matecki**[2,4], **Alain Lacampagne**[3,4], and **Andrew R. Marks**[1,5]

[1] Clyde and Helen Wu Center for Molecular Cardiology, Departments of Physiology and Cellular Biophysics, and Medicine, Columbia University College of Physicians and Surgeons, New York, NY 10032

[2] Institut National de la Santé et de la Recherche Médicale, ERI25

[3] Institut National de la Santé et de la Recherche Médicale, U 637

[4] Unité de Formation et de Recherche de Médecine, Université Montpellier 1, F-34295 Montpellier, France

Abstract

Duchenne muscular dystrophy (DMD) is characterized by progressive muscle weakness and early death resulting from dystrophin deficiency. Loss of dystrophin results in disruption of a large dystrophin glycoprotein complex (DGC) leading to pathologic calcium (Ca^{2+})-dependent signals that damage muscle cells [1–5]. We have identified a structural and functional defect in the sarcoplasmic reticulum (SR) Ca^{2+} release channel/ryanodine receptor (RyR1) in the *mdx* mouse model of muscular dystrophy that may contribute to altered Ca^{2+} homeostasis in dystrophic muscles. RyR1 isolated from *mdx* skeletal muscle exhibited an age-dependent increase in S-nitrosylation coincident with dystrophic changes in the muscle. RyR1 S-nitrosylation depleted the channel complex of FKBP12 (or "calstabin1" for calcium channel stabilizing binding protein) resulting in "leaky" channels. Preventing calstabin1 depletion from RyR1 using S107, a compound that binds to the RyR1 channel and enhances the binding affinity of calstabin1 to the nitrosylated channel, inhibited SR Ca^{2+} leak, reduced biochemical and histologic evidence of muscle damage, improved muscle function and increased exercise performance in *mdx* mice. Thus, SR Ca^{2+} leak via RyR1 due to S-nitrosylation of the channel and calstabin1 depletion likely contributes to muscle weakness in muscular dystrophy and preventing the RyR1-mediated SR Ca^{2+} leak may provide a novel therapeutic approach.

[5]To whom correspondence should be addressed at: arm42@columbia.edu, Phone (212) 305-0270, Fax (212) 305-3690.

Note: Supplementary information is available on the Nature Medicine website.

AUTHOR CONTRIBUTIONS

A.M.B. conducted experiments and wrote the manuscript, S.R. performed biochemistry experiments, C.C. assisted with animal experiments, M.M. performed immunohistochemistry, X.L. and L.R. assisted with histology, S.M. and S.M. performed muscle and calcium experiments, A.R.M. conceived, designed and directed the project, analyzed data, and wrote the final version of the manuscript.

DMD, the most common X-linked disorder (affecting 1 in 3,500 male births), typically results in death due to respiratory or cardiac failure by age 30 [6]. Loss of dystrophin leads to disruption of the DGC that bridges the sarcolemmal surface and connects the cytoskeleton and contractile apparatus to the extracellular matrix and basement membrane [7,8]. Cytoplasmic calcium ($[Ca^{2+}]_{cyt}$) homeostasis in dystrophic fibers is abnormal [1,3,9]. Disruption of the DGC impairs sarcolemmal membrane integrity and results in increased influx of Ca^{2+} into the muscle across the sarcolemma which has been attributed to Ca^{2+} "leak" channels in the plasma membrane [5], microscopic membrane tears [3,10], mechanosensitive Ca^{2+} channels [11], or store-operated Ca^{2+} channels activated by SR Ca^{2+} depletion [12,13]. Elevated $[Ca^{2+}]_{cyt}$ is implicated in the pathophysiology of protein degradation in *mdx* muscle [4], and cell death [14]. A downstream effect of elevated $[Ca^{2+}]_{cyt}$ is activation of calpains (Ca^{2+}-dependent neutral proteases) [15]. Transgenic expression of calpastatin in the dystrophic mouse partially rescues myofiber damage [16]. It has been proposed that elevated $[Ca^{2+}]_{cyt}$ contributes to myofiber death at a rate that cannot be compensated for by recruitment of progenitor (satellite) muscle cells and regeneration and differentiation of new muscle cells [3]. SR Ca^{2+} reuptake is slowed in *mdx* myofibers and an SR Ca^{2+} leak of uncertain etiology has been reported [5,11,17]. The rate of Ca^{2+} sparks in dystrophic fibers is increased, further suggesting that a defect in SR Ca^{2+} release may be present in muscular dystrophy [18].

An approximately 80% reduction in nitric oxide synthase (NOS) mRNA and protein have been reported in dystrophin-deficient muscle [19,20] and has been implicated in the pathophysiology of muscular dystrophy [21]. RyR1 contains multiple cysteine residues [22] that can be modified at physiological pH by either S-nitrosylation or S-glutathionylation [23–25]. cGMP-independent, NO-mediated regulation of RyRs increases channel activity in vesicles and in single channel measurements [22]. Exogenous S-nitrosylation of RyR1 has been shown to reduce the affinity of calstabin1 binding to SR triads [26].

We hypothesized that defects in the RyR1 macromolecular complex may contribute to the abnormalities in $[Ca^{2+}]_{cyt}$ in muscular dystrophy. To test this hypothesis, we assessed the composition of the RyR1 macromolecular complex [27,28] from hind limb extensor digitorum longus (EDL) muscle of *mdx* mice. Histologic evidence of muscular dystrophy is evident at 35 days of age. In mice at this age there was a significant increase in S-nitrosylation of cysteine residues in RyR1 from *mdx* mice compared to age matched WT littermates (Fig. 1a,b). Increased RyR1 S-nitrosylation correlated with depletion of calstabin1 from the RyR1 complex (Fig. 1a,b). We observed no differences in S-nitrosylation, PKA phosphorylation of RyR1 (at Ser2844), or calstabin1 bound to the RyR1 complex between *mdx* mice and WT littermates at 7 and 21 days of age (Fig. 1a,b). Moreover, there was no increase in PKA phosphorylation of RyR1 at Ser2844 in *mdx* mice at any age examined (Fig. 1a,b). Total levels of calstabin1 in whole muscle lysate were not altered in *mdx* muscle at any age, indicating that reduced calstabin1 binding to RyR1 is due to reduced binding to RyR1 rather than altered expression (Fig 1c). Immunoprecipitation of RyR1 was specific and efficient, leaving little RyR1 in the voided fraction (Supplemental Fig. 1). Thus, RyR1 S-nitrosylation and calstabin1 depletion correlated with muscular dystrophy in *mdx* mice.

Exogenous S-nitrosylation of RyR1 using NO donors resulted in depletion of calstabin1 from the channel (Fig. 2a), as previously reported [26]. To identify the basis for the increased S-nitrosylation of RyR1, we determined levels of nitric oxide synthase isoforms by immunoblotting WT and *mdx* EDL muscles for iNOS, eNOS, and nNOS expression (Fig. 2b). iNOS levels were significantly increased in EDL muscles from *mdx* mice 35 days and older and were essentially undetectable in WT muscle. eNOS levels were decreased in *mdx* skeletal muscle compared to WT littermates. nNOS expression was decreased in *mdx* tissue. RyR1 and iNOS (but not eNOS) co-immunoprecipitated from *mdx* EDL muscle (Fig. 2c,d), iNOS was not detected in immunoprecipitates from WT muscle using either anti-RyR1 or anti-iNOS antibodies. iNOS immunoprecipitated with RyR1 at 35 and 180 days of age (Fig. 2e). Moreover, iNOS co-localized with RyR1 in *mdx* EDL muscle, whereas iNOS was not detected in WT EDL muscle (Fig. 2f). These data suggest that iNOS is a component of the RyR1 macromolecular complex in *mdx* mice, but not in WT.

We have reported that RyR Ca^{2+} release channel stabilizers, which we propose calling "rycals", inhibit depletion of calstabin1 from PKA hyperphosphorylated RyR1 [28,29]. We hypothesized that treatment with S107, a stable cell-permeable rycal [28], begun as early as possible in *mdx* mice, would reduce the RyR1-mediated SR Ca^{2+} leak induced by S-nitrosylation of RyR1 and calstabin1 depletion, and partially protect against muscle damage due to $[Ca^{2+}]_{cyt}$-mediated calpain activation.

We randomized four to five week old male *mdx* mice to treatment with either S107 (20 μg hr^{-1}) or vehicle (H_20) via a subcutaneous osmotic pump. We assessed forelimb grip strength after two weeks of treatment. There was significant improvement in grip strength in the S107 treated group ($n = 14$, $P < 0.001$ vs. WT controls, $n = 9$, and vehicle controls, $n = 14$,) (Fig. 3a). Normalized for BW, grip strength was significantly improved in *mdx* mice treated with S107 ($P < 0.01$, t-test analysis of two independent, pair-matched, blinded cohorts) (Fig. 3b). Serum creatine kinase (CK), a marker of muscle necrosis, was significantly reduced by S107 treatment in *mdx* mice, suggesting a reduction in muscle damage (Fig. 3c). Calpain concentration in the EDL hind limb muscle (determined by measuring activatable calpain in the muscle) was also reduced by S107 treatment, suggesting that inhibition of RyR1-mediated SR Ca^{2+} leak may reduce Ca^{2+}-activated proteolytic enzyme activity leading to protection of dystrophic muscle against damage (Fig. 3d). Eccentric (lengthening) exercise such as downhill running is particularly difficult for *mdx* mice [30]. S107 treated *mdx* mice completed a 30-minute downhill run at a higher rate than vehicle treated mice (9/11 vs. 3/10, $P < 0.05$). CK was reduced in these *mdx* mice by treatment with S107 (6,200 vs. 13,300 UL^{-1}, $P < 0.05$), providing further evidence that S107 can improve function and reduce CK leak in *mdx* muscle. Calpain activation in the EDL hind limb muscle in these *mdx* mice was reduced by S107 treatment (1,250 vs. 2,100 U μg^{-1}, $P < 0.05$), suggesting that stabilization of RyR1 reduced Ca^{2+} leak and Ca^{2+}-activated proteolytic enzyme activity. S107 prevented depletion of calstabin1 from S-nitrosylated RyR1 without affecting PKA phosphorylation of nitrosylation of the channel, or another component of the RyR1 complex PDE4D3 (Fig. 3e,f). NOS isoform expression was not altered by S107 treatment (Fig. 3g).

Treatment of *mdx* mice with S107 via osmotic pump beginning at 4–5 weeks of age for up to 4 weeks resulted in improvement in the histological hallmarks of dystrophy. In the tibialis

anterior hind limb muscle, there was a reduction in Evans Blue Dye (EBD) positive fibers, 12.1 ± 2.8% in *mdx* treated with S107 ($n = 3$) vs. 26.3 ± 5.3 in vehicle treated *mdx* ($n = 3$, $P < 0.05$) (Fig. 3h). In diaphragmatic muscle, there were reduced central nuclei (28% reduction in *mdx* treated with S107, $P < 0.05$), EB positive muscle fibers (50% reduction in *mdx* treated with S107, $P < 0.05$), and increased fiber cross-sectional area (32% increase in *mdx* treated with S107, $P < 0.05$) in the *mdx* mice treated with S107 ($n = 5$) compared to *mdx* mice treated with vehicle alone ($n = 4$) (Fig. 3i). These improvements in the histology of the dystrophic muscles correlated with the improvement in muscle function and reduction in CK and calpain (Fig. 3a–d).

We subjected EDL to eccentric contraction and determined the resulting force deficit, which we defined as the percentage decline in isometric force after one eccentric contraction. The latter served as a functional indicator of contraction-induced mechanical injury to dystrophic muscle as previously reported [30]. We recorded force production during a 100-Hz tetanus train *in situ* first in combination with an eccentric lengthening (to 115% of initial length) followed after 1 min rest by a 100-Hz tetanus train without eccentric stress (Fig. 4a). Eccentric contraction in *mdx* muscle resulted in significant reduction in force production compared to control muscles. In mice treated for 7–8 days with S107 in the drinking water (~37.5 mg kg^{-1} day^{-1}), this deficit in force production after one eccentric contraction was reduced to control value (Fig. 4b). We thus hypothesized that alterations and/or damage occurring during eccentric contractions in *mdx* mice were linked to defective RyR1 channel function, specifically a leak of SR Ca^{2+} via RyR1. To further test this hypothesis we analyzed spontaneous Ca^{2+} release events, or Ca^{2+} sparks, in control WT and in *mdx* mice after one episode of mild eccentric contraction. Ca^{2+} spark frequency was significantly increased in muscle fibers from *mdx* mice compared to control animals (Fig. 4c–f). Other spatio-temporal properties of the sparks including amplitude, rise time, decay time constant or spatial spread (full width at half maximum) were not different between the two groups (data not shown). Of note there was no difference in spatio-temporal Ca^{2+} spark properties between control and *mdx* mice without mechanical stress (i.e. eccentric contraction) as well as control muscle with and without eccentric contraction (data not shown). Thus, inhibiting calstabin1 depletion from the RyR1 complex using S107 treatment reduced the SR Ca^{2+} leak via RyR1 manifested as a reduction in Ca^{2+} spark frequency in the muscle of *mdx* mice treated with the rycal (Fig. 4e,f).

We next tested whether treatment with S107 could improve voluntary exercise by placing a wheel in the mouse cage for five days to acclimate the mice then measuring time spent on the wheel, average and maximal velocities over 72 hours. *Mdx* mice treated with S107 spent significantly more time on the wheel and achieved ~50% higher maximal velocities compared to *mdx* mice treated with vehicle alone (Fig. 4g). In addition, S107 treatment significantly increased specific force (Fig. 4h) and resistance to fatigue determined as relative force during tetanic stimulation (Fig. 4i) in *mdx* muscle compared to vehicle treated *mdx* controls determined by in situ force measurements of the EDL.

Taken together our data show that RyR1 Ca^{2+} release channels are leaky in *mdx* skeletal muscle (Fig. 4d) due to RyR1 hypernitrosylation (Fig. 1a,b) which depletes the RyR1 channel complex of the stabilizing subunit calstabin1 (FKBP12) (Fig. 1a,b). The

hypernitrosylation of RyR1 was associated with a significant increase in the levels of iNOS in the *mdx* muscle (Fig. 2), and the formation of an iNOS-RyR1 complex (Fig. 2c,e). The RyR1-mediated intracellular Ca^{2+} leak was associated with increased concentrations of the Ca^{2+}-activated protease calpain in *mdx* muscle (Fig. 3d) that may contribute to the observed muscle damage (Fig. 3c,g), impaired muscle force (Fig. 4b,h,i) and decreased exercise capacity in *mdx* mice (Fig. 4g). We have previously shown that calstabin1 (FKBP12) stabilizes the closed state of individual RyR1 channels [31] and mediates "coupled gating" between multiple RyR1 channels [32]. Both stabilization of the RyR1 closed state and coupled gating likely play roles in preventing aberrant SR Ca^{2+} leak through RyR1 channels. Treatment with a drug S107 that inhibits depletion of calstabin1 (FKBP12) from hypernitrosylated RyR1 channels in dystrophic muscle (Fig. 3e), reduced pathologic SR Ca^{2+} leak (Fig. 4c–f), calpain activation (Fig. 3d), protected against muscle damage (Fig. 3d), improved muscle force, reduced fatigue (Fig. 4a,b), improved grip strength (Fig. 3a,b) and voluntary exercise (Fig. 4g) in *mdx* mice.

Remarkably these improvements are observed within one (improved exercise capacity) to four weeks (histologic improvement) of S107 treatment, which is considerably faster than most genetic therapies. This suggests that the RyR1-mediated intracellular Ca^{2+} leak is downstream of the genetic defects that cause MD (e.g. dystrophin deficiency).

It has been suggested that RyR1 channel function may be regulated by S-nitrosylation but to date the physiological consequences of this form of regulation *in vivo* have not been well understood. Neuronal nitric oxide synthase (nNOS) is the principal source of nitric oxide in skeletal muscle. It is localized at the plasma membrane, where an N-terminal GLGF motif binds to the dystrophin complex via an interaction with syntrophin [19],[33]. The disruption of the DGC in DMD results in a selective loss of nNOS catalytic activity that is associated with its down-regulation at the transcriptional level [19],[20]. Recently, Campbell and colleagues showed that reduced sarcolemmal-localized nNOS is linked to decreased activity following mild exercise (10 min downhill run) in mouse models including the *mdx* mice, and that treatment with a PDE5 inhibitor increased activity following mild exercise [34]. In contrast, iNOS is significantly increased in the skeletal muscle of both DMD patients and *mdx* mice, and rescue of the *mdx* phenotype by adenoviral-mediated dystrophin or utrophin expression normalizes iNOS activity [35]. The concurrent down regulation of nNOS and up regulation of iNOS suggest that the latter could be a compensatory response, but that differences in subcellular localization of the two NOS isoforms could account for some of the pathology observed in the *mdx* mice including the leaky RyR1 channels (associated with increased iNOS in the RyR1 complex) reported in the present study and the post-exercise vasoconstriction (associated with loss of nNOS in the DGC) reported by Kobayashi et al [34]. Increased nitrosylative stress in the RyR1 complex during muscular dystrophy and increased Ca^{2+} influxes across the plasma membrane due to the disruption of the DGC may both activate RyR1 channels, especially since the RyR1 channel is depleted of the stabilizing subunit calstabin1 (FKBP12) in *mdx* mouse skeletal muscle rendering it particularly sensitive to Ca^{2+}-mediated activation.

Therapeutic strategies for muscular dystrophy have consisted primarily of gene therapy to replace dystrophin [36], up regulation of the dystrophin homologue utrophin [37], acceleration

of the rate of muscle regeneration [38,39], and exon skipping achieved via viral mediated expression of antisense sequences linked to a modified U7 small nuclear RNA [40]. Stabilizing RyR1 by inhibiting SR Ca^{2+} leak using a small molecule may provide an additional strategy that protects against muscle damage and improves function.

METHODS

Animals and treatment with S107

We obtained C57BL/10ScSc-Dmd^{mdx}/J, referred to as *mdx* (stock #001801) and C57BL/6J, referred to as WT, from Jackson Laboratories and bred to obtain male *mdx* and WT littermate controls. We randomized mice to treatment with either S107 or vehicle (H_2O). In some experiments we implanted osmotic pumps (Alzet Model 1004, 100 μl total volume, 0.11 μl hr^{-1} delivery for ~28 days, Durect) filled with H_2O or S107 (80 μg $μl^{-1}$ diluted in H_2O) subcutaneously on the dorsal surface of each mouse by a horizontal incision at the neck for 2 to 4 weeks as indicated. In other experiments we added S107 to the drinking water (final concentration, 0.25 mg ml^{-1}) as indicated. Mice drank ~3 ml d^{-1} (water consumption was variable and we recorded water bottle and body weight to monitor consumption) for a daily dose of ~0.75 mg (~37.5 mg kg^{-1} d^{-1}) which resulted in a plasma concentration of ~35 ± 21 ng ml^{-1} (~140 nM, determined in the early morning to reflect higher water consumption during the night). We conducted all experiments in accordance with protocols approved by the Institutional Animal Care and Use Committee of Columbia University and Université Montpellier. Individuals blinded to the treatment status of the animals conducted all studies involving drug treatments, including analyses of function and histologic sections.

Immunoblotting

We incubated membranes for 1–2 hr at RT with the following primary antibodies: RyR1 (RyR1-1327), a rabbit polyclonal antibody raised against a KLH-conjugated peptide based on the mouse skeletal RyR1 corresponding to amino acids 1327–1339 (CAEPDTDYENLRRS), with a cysteine residue added to the amino terminus, affinity purified using the antigenic peptide, specifically recognizes RyR1 (Supplementary Fig. 1 online) and does not react with RyR2 or RyR3 used at 1:2500–1:5000 dilution for immunoblotting and 1:250 for immunoprecipitation; antibody to calstabin (1:2500 in blocking buffer); antibody to phospho-RyR2-pSer2809 (1:5000), which detects PKA-phosphorylated mouse RyR1-pSer2844 and RyR2-pSer2808; antibody to Cys-NO (1:1000, Sigma), antibody to PDE4D3 (1:1000), antibodies to iNOS (1:2000), eNOS, or nNOS (1:1000, VWR).

Grip Strength

We assessed forelimb grip strength after 2 wks of treatment with S107 or vehicle. We allowed each mouse to grab a hold bar attached to a force transducer that records peak force generated as the rodent is pulled by the tail horizontally away from the bar (Model #303500-M/C-1, TSE Systems). We performed five consecutive pulls separated by 15 sec pauses between each pull. We averaged the middle three pulls to calculate the absolute grip strength

(in ponds, 1 pond = ~9.8 mN) which we divided by the mouse's body weight (BW) in grams.

Creatine Kinase and Calpain Assay

We determined CK levels based on the absorbance change min^{-1} using a commercial assay (Pointe Scientific, Inc. per manufacturer's instructions). We diluted muscle homogenates (EDL) to a final concentration of 600 μg ml^{-1} and we determined the calpain activity in the homogenate using a commercial assay as per manufacturer's instructions (Calbiochem).

Measurement of EDL resistance to contraction-induced mechanical stress

We anesthetized mice (male, 40 days old) with 130 mg/kg ketamine and 20 mg kg^{-1} xylazine, and immobilized in the supine position on a surgical platform at 37 °C. We exposed the anterior region of the lower hind limb from the ankle to just above the knee. We isolated the distal tendon of the tibialis anterior (TA) and tied it with 4-0 nylon suture to the lever arm of a force transducer/length servomotor system (model 305B dual mode; Aurora Scientific Inc.), which we mounted on a mobile micrometer stage to allow fine incremental adjustments of muscle length. We kept exposed muscles moist with a 37°C isotonic saline drip. We stimulated the EDL indirectly via an electrode placed on the belly of the TA.

Calcium sparks

We acquired fluorescence images using a Zeiss LSM 510 META NLO confocal system equipped with a three-point 63X water immersion objective, NA=1.2) operated in line-scan mode (*x* vs. *t*, 1.5 ms per line, 3000 lines per scan) along the longitudinal axis of the fibers. We excited Fluo-3 at 488 nm with an Argon laser, and recorded the emitted fluorescence at 525 nm.

Voluntary exercise measurements

We evaluated voluntary exercise using a wheel (15×40×15 cm cage with a 5.5 cm×12 cm wheel) placed in the cage.

Statistical analysis

We presented data as mean ± SEM. We employed an independent t-test with a significance level of 0.05 to test differences between *mdx* and WT. When we made multiple comparisons between WT, *mdx*-veh, and *mdx*-S107 we used a Bonferroni adjustment with a pair-wise significance level of 0.015.

Supplementary Material

Refer to Web version on PubMed Central for supplementary material.

Acknowledgments

This work was supported in part by a grant from the Leducq Foundation. A. Marks and S. Reiken are consultants for ARMGO Pharma, Inc., a start-up company targeting RyR1 to reduce SR Ca^{2+} leak. The authors thank J. Shan for assistance with analyses of histologic sections and J. Fauconnier for help with voluntary exercise measurements in mice.

References

1. Bodensteiner JB, Engel AG. Intracellular calcium accumulation in Duchenne dystrophy and other myopathies: a study of 567,000 muscle fibers in 114 biopsies. Neurology. 1978; 28:439–446. [PubMed: 76996]
2. Glesby MJ, Rosenmann E, Nylen EG, Wrogemann K. Serum CK, calcium, magnesium, and oxidative phosphorylation in mdx mouse muscular dystrophy. Muscle Nerve. 1988; 11:852–856. [PubMed: 3173410]
3. Blake DJ, Weir A, Newey SE, Davies KE. Function and genetics of dystrophin and dystrophin-related proteins in muscle. Physiol Rev. 2002; 82:291–329. [PubMed: 11917091]
4. Turner PR, Westwood T, Regen CM, Steinhardt RA. Increased protein degradation results from elevated free calcium levels found in muscle from mdx mice. Nature. 1988; 335:735–738. [PubMed: 3173492]
5. Fong PY, Turner PR, Denetclaw WF, Steinhardt RA. Increased activity of calcium leak channels in myotubes of Duchenne human and mdx mouse origin. Science. 1990; 250:673–676. [PubMed: 2173137]
6. Hoffman EP, Brown RH, Kunkel LM. Dystrophin: The protein product of the duchenne muscular dystrophy locus. Cell. 1987; 51:919–928. [PubMed: 3319190]
7. Bonilla E, et al. Duchenne muscular dystrophy: Deficiency of dystrophin at the muscle cell surface. Cell. 1988; 54:447–452. [PubMed: 3042151]
8. Matsumura K, Ervasti JM, Ohlendieck K, Kahl SD, Campbell KP. Association of dystrophin-related protein with dystrophin-associated proteins in mdx mouse muscle. Nature. 1992; 360:588–591. [PubMed: 1461282]
9. Yeung EW, et al. Effects of stretch-activated channel blockers on $[Ca^{2+}]_i$ and muscle damage in the mdx mouse. J Physiol. 2005; 562:367–380. [PubMed: 15528244]
10. Bradley WG, Fulthorpe JJ. Studies of sarcolemmal integrity in myopathic muscle. Neurology. 1978; 28:670–677. [PubMed: 79157]
11. Franco A Jr, Lansman JB. Calcium entry through stretch-inactivated ion channels in mdx myotubes. Nature. 1990; 344:670–673. [PubMed: 1691450]
12. Vandebrouck C, Martin D, Colson-Van Schoor M, Debaix H, Gailly P. Involvement of TRPC in the abnormal calcium influx observed in dystrophic (mdx) mouse skeletal muscle fibers. J Cell Biol. 2002; 158:1089–1096. [PubMed: 12235126]
13. Boittin FX, et al. Ca^{2+}-independent phospholipase A2 enhances store-operated Ca^{2+} entry in dystrophic skeletal muscle fibers. J Cell Sci. 2006; 119:3733–3742. [PubMed: 16926189]
14. Robert V, et al. Alteration in calcium handling at the subcellular level in mdx myotubes. J Biol Chem. 2001; 276:4647–4651. [PubMed: 11029464]
15. Spencer MJ, Croall DE, Tidball JG. Calpains are activated in necrotic fibers from mdx dystrophic mice. J Biol Chem. 1995; 270:10909–10914. [PubMed: 7738032]
16. Spencer MJ, Mellgren RL. Overexpression of a calpastatin transgene in mdx muscle reduces dystrophic pathology. Hum Mol Genet. 2002; 11:2645–2655. [PubMed: 12354790]
17. Turner PR, Fong PY, Denetclaw WF, Steinhardt RA. Increased calcium influx in dystrophic muscle. J Cell Biol. 1991; 115:1701–1712. [PubMed: 1661733]
18. Wang X, et al. Uncontrolled calcium sparks act as a dystrophic signal for mammalian skeletal muscle. Nat Cell Biol. 2005; 7:525–530. [PubMed: 15834406]
19. Brenman JE, Chao DS, Xia H, Aldape K, Bredt DS. Nitric oxide synthase complexed with dystrophin and absent from skeletal muscle sarcolemma in Duchenne muscular dystrophy. Cell. 1995; 82:743–752. [PubMed: 7545544]
20. Chang WJ, et al. Neuronal nitric oxide synthase and dystrophin-deficient muscular dystrophy. Proc Natl Acad Sci U S A. 1996; 93:9142–9147. [PubMed: 8799168]
21. Wehling M, Spencer MJ, Tidball JG. A nitric oxide synthase transgene ameliorates muscular dystrophy in mdx mice. J Cell Biol. 2001; 155:123–131. [PubMed: 11581289]
22. Xu L, Eu JP, Meissner G, Stamler JS. Activation of the cardiac calcium release channel (ryanodine receptor) by poly-S-nitrosylation. Science. 1998; 279:234–237. [PubMed: 9422697]

23. Sun J, Xin C, Eu JP, Stamler JS, Meissner G. Cysteine-3635 is responsible for skeletal muscle ryanodine receptor modulation by NO. PNAS. 2001; 98:11158–11162. [PubMed: 11562475]
24. Aracena P, Sanchez G, Donoso P, Hamilton SL, Hidalgo C. S-Glutathionylation Decreases Mg^{2+} Inhibition and S-Nitrosylation Enhances Ca^{2+} Activation of RyR1 Channels. J Biol Chem. 2003; 278:42927–42935. [PubMed: 12920114]
25. Sun J, Xu L, Eu JP, Stamler JS, Meissner G. Nitric Oxide, NOC-12, and S-nitrosoglutathione modulate the skeletal muscle calcium release channel/ryanodine Receptor by different mechanisms. An allosteric function for O_2 in S-nitrosylation of the channel. J Biol Chem. 2003; 278:8184–8189. [PubMed: 12509428]
26. Aracena P, Tang W, Hamilton S, Hidalgo C. Effects of S-glutathionylation and S-nitrosylation on calmodulin binding to triads and FKBP12 binding to type 1 calcium release channels. Antioxid Redox Signal. 2005; 7:870–881. [PubMed: 15998242]
27. Marx SO, et al. Phosphorylation-dependent regulation of ryanodine receptors: a novel role for leucine/isoleucine zippers. J Cell Biol. 2001; 153:699–708. [PubMed: 11352932]
28. Bellinger A, Reiken SR, Dura M, Murphy P, Deng S-X, Neiman D, Lehnart S, Samaru M, LaCampagne A, Marks AR. Remodeling of ryanodine receptor complex causes “leaky” channels: a molecular mechanism for decreased exercise capacity. PNAS. 2008; 105:2198–2202. [PubMed: 18268335]
29. Wehrens XH, et al. Enhancing calstabin binding to ryanodine receptors improves cardiac and skeletal muscle function in heart failure. PNAS. 2005; 102:9607–9612. [PubMed: 15972811]
30. Vilquin JT, et al. Evidence of mdx mouse skeletal muscle fragility in vivo by eccentric running exercise. Muscle Nerve. 1998; 21:567–576. [PubMed: 9572235]
31. Brillantes AB, et al. Stabilization of calcium release channel (ryanodine receptor) function by FK506-binding protein. Cell. 1994; 77:513–523. [PubMed: 7514503]
32. Marx SO, Ondrias K, Marks AR. Coupled gating between individual skeletal muscle Ca^{2+} release channels (ryanodine receptors). Science. 1998; 281:818–821. [PubMed: 9694652]
33. Kameya S, et al. alpha 1-Syntrophin gene disruption results in the absence of neuronal-type nitric-oxide synthase at the sarcolemma but does not induce muscle degeneration. J Biol Chem. 1999; 274:2193–2200. [PubMed: 9890982]
34. Kobayashi YM, et al. Sarcolemma-localized nNOS is required to maintain activity after mild exercise. Nature. 2008
35. Louboutin JP, Rouger K, Tinsley JM, Halldorson J, Wilson JM. iNOS expression in dystrophinopathies can be reduced by somatic gene transfer of dystrophin or utrophin. Molecular Medicine. 2001; 7:355–364. [PubMed: 11474581]
36. Gregorevic P, et al. rAAV6-microdystrophin preserves muscle function and extends lifespan in severely dystrophic mice. Nat Med. 2006; 12:787–789. [PubMed: 16819550]
37. Krag TOB, et al. Heregulin ameliorates the dystrophic phenotype in mdx mice. PNAS. 2004; 101:13856–13860. [PubMed: 15365169]
38. Zaccagnini G, et al. p66ShcA and oxidative stress modulate myogenic differentiation and skeletal muscle regeneration after hindlimb ischemia. J Biol Chem. 2007
39. Khurana TS, Davies KE. Pharmacological strategies for muscular dystrophy. Nat Rev Drug Discov. 2003; 2:379–390. [PubMed: 12750741]
40. Goyenvalle A, et al. Rescue of dystrophic muscle through U7 snRNA-mediated exon skipping. Science. 2004; 306:1796–1799. [PubMed: 15528407]

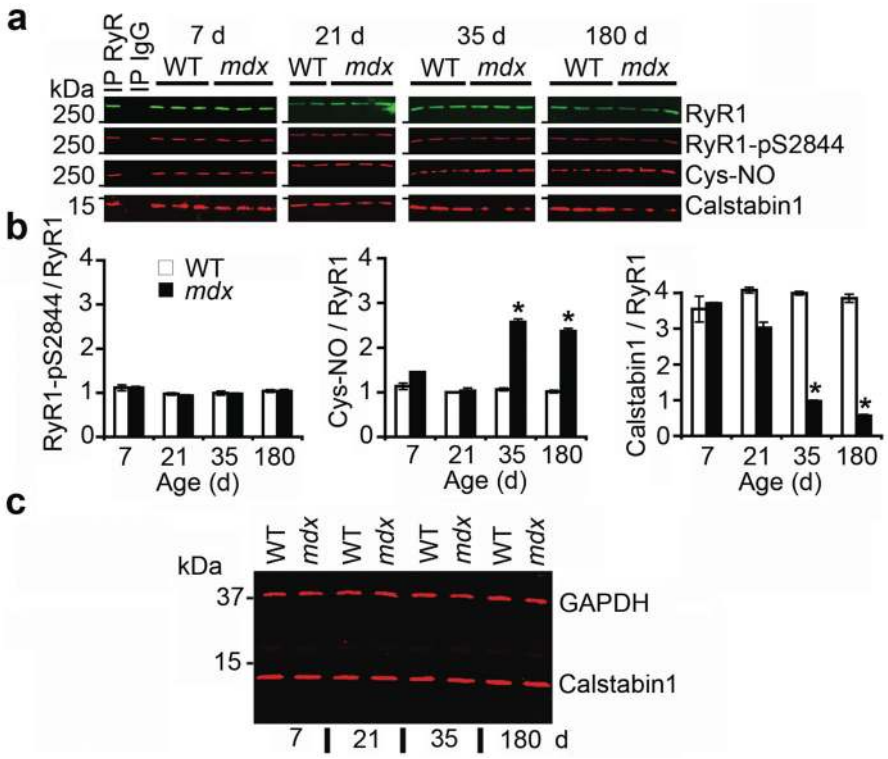

Figure 1. RyR1 is S-nitrosylated and depleted of calstabin1 in *mdx* mice

(**a**) RyR1 was immunoprecipitated from EDL muscle of *mdx* mice and WT littermates at 7, 21, 35, and 180 days after birth and immunoblotted for RyR1, RyR1 PKA phosphorylated at Ser2844 (RyR1-pS2844), S-nitrosylation of cysteine residues on RyR1 (Cys-NO), and calstabin1 bound to RyR1. Positive and negative control (IgG) immunoprecipitation are shown for 7 day WT hearts. Blots are representative of three independent experiments. (**b**) Quantification of RyR1 PKA phosphorylation, RyR1 S-nitrosylation, and bound calstabin1 relative to total RyR1. Data presented as mean ± S.E.M. *, $P < 0.05$, t-test. (**c**) Immunoblot for total calstabin1 in whole EDL muscle lysate (25 μg) from WT and mdx mice at indicated ages. GAPDH was used as a loading control.

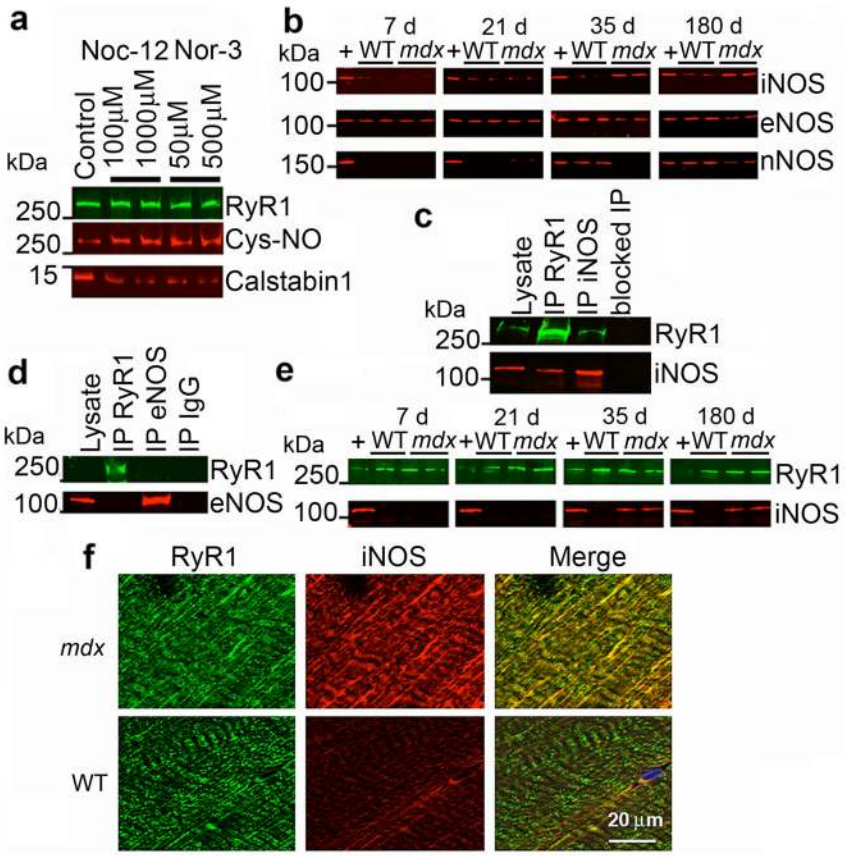

Figure 2. iNOS co-immunoprecipitates and co-localizes with RyR1 and S-nitrosylation of RyR1 depletes the channel of calstabin1

(**a**) *In vitro* S-nitrosylation of skeletal SR microsomes with NO donors Nor-3 or Noc-12 results in depletion of calstabin1 from immunoprecipitated RyR1. (**b**) Immunoblot of expression of three NOS isoforms (iNOS, eNOS, and nNOS) from WT and *mdx* whole muscle lysates at the indicated ages. (**c**) Co-immunoprecipitation of RyR1 and iNOS. 50 µg of *mdx* EDL lysate was used as positive control. RyR1 and iNOS separately immunoprecipitated from 250 µg of *mdx* muscle lysate and probed for RyR1 and iNOS. Antibody against RyR was pre-incubated with 100-fold excess antigenic peptide prior to immunoprecipitation (blocked IP RyR). (**d**) Immunoprecipitation-immunoblotting of RyR1 and eNOS from *mdx* lysate. IgG control immunoprecipitation shown at right. (**e**) RyR1 was immunoprecipitated from WT and *mdx* EDL lysates at indicated ages and immunoblotted for RyR1 and iNOS. (f) Immunohistochemistry showing co-localization of RyR1 and iNOS in murine skeletal muscle (EDL) from *mdx* but not WT mice. Scale bar in lower right panel applies to all six panels.

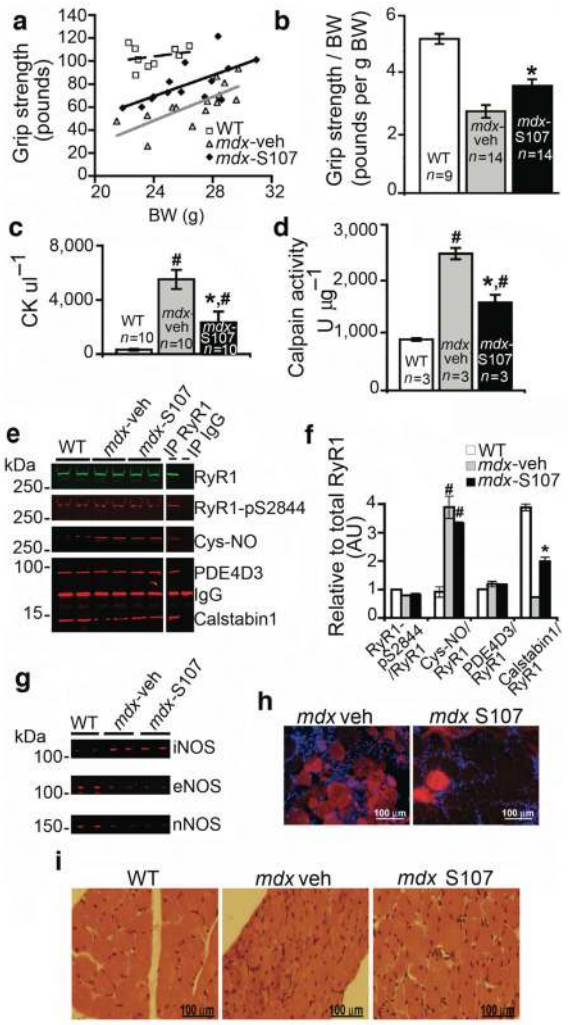

Figure 3. Preventing calstabin1 depletion from the RyR1 complex with S107 improves grip strength and reduces muscle damage

(**a**) We determined forelimb grip strength in sedentary mice after two weeks of treatment with S107 administered via an osmotic pump as described in the methods. (*mdx*-S107, n = 14, black diamond), vehicle (*mdx*-vehicle, n = 14, grey triangle), WT (n = 9, open square) mice. Data are presented as a scatter plot of absolute grip strength (ponds) versus body weight (BW, g). Least square fit lines are overlaid. (**b**) Grip strength normalized to BW. *, P < 0.015, t-test with Bonferroni adjustment, *mdx*-S107 vs *mdx*-veh. (**c**) CK levels (#, P < 0.015 vs. WT; *, P < 0.015 *mdx*-S107 vs. *mdx*-veh; t-tests with Bonferroni adjustment). (**d**) EDL tissue calpain activity (#,P < 0.015 vs. WT; *, P < 0.015 *mdx*-S107 vs. *mdx*-veh; t-tests with Bonferroni adjustment). (**e**) RyR1 immunoprecipitated from hind limb EDL muscle immunoblotted for total RyR1, RyR1-pS2844, Cys-NO, PDE4D3 and calstabin1 bound to RyR1. (**f**) Quantification of (e) showing levels of indicated proteins normalized to the total amount of RyR1 (AU, arbitrary units). Data presented as mean ± S.E.M. (#, P < 0.015 for RyR1-Cys-NO, *mdx* vs. WT; *, P < 0.015, for calstabin1 binding to RyR1, *mdx* treated with S107 vs. *mdx* treated with vehicle). (**g**) Immunoblot for iNOS, eNOS, and nNOS in EDL whole muscle lysates. (**h**) Representative images of DAPI stained 10 µm TA sections from

mice injected with 100 μl of 1% Evans Blue Dye intraperitoneally 24 hrs prior to sacrifice. S107 treatment was begun at 35 days of age and continued for 4 wks via osmotic pump. (**i**) Representative H&E stained images from diaphragm.

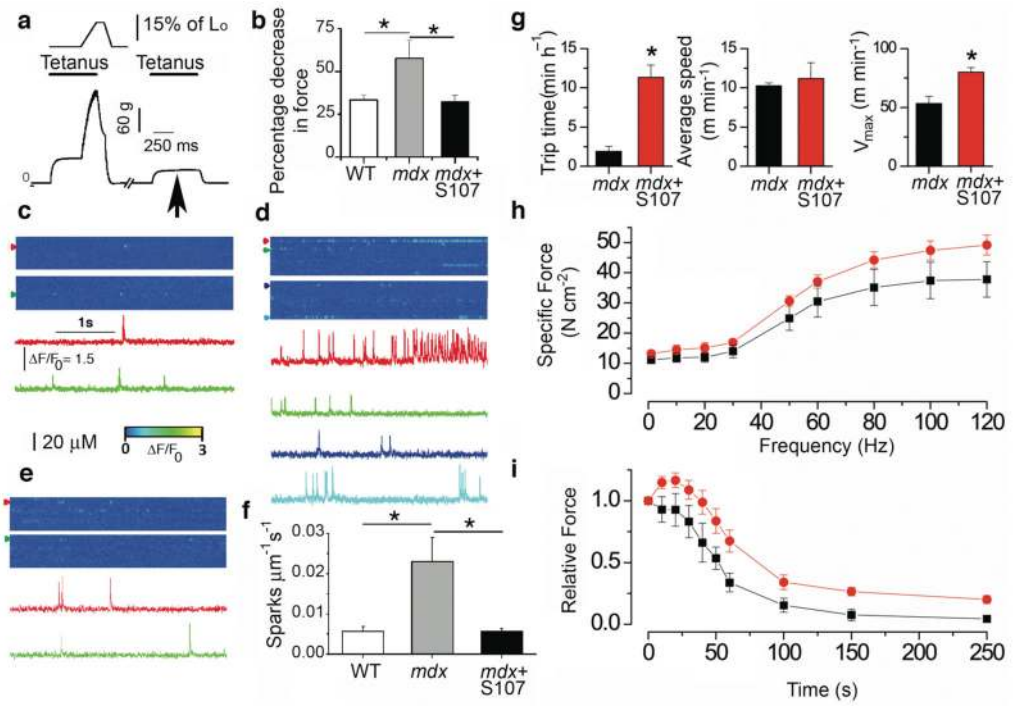

Figure 4. Preventing RyR1 leak with S107 reduces Ca^{2+} leak, enhances muscle force, and voluntary exercise in *mdx* mice

(**a**) Isometric and eccentric force production in EDL muscle *in situ* in anesthetized mice (Supplementary Methods, online). Typical recording from an *mdx* mouse EDL muscle (bottom graph) indicating a decline in force production during tetanus following mechanical stress (arrow). (**b**) Effect of oral S107 on decrease in force production in *mdx* mice (S107, 0.25 mg ml^{-1}, in the drinking water for 10 days prior to testing, $n = 5$ for each group). Spontaneous Ca^{2+} sparks recorded in EDL muscles from: WT (**c**), vehicle treated *mdx* (**d**), and S107 treated *mdx* mice (**e**). Representative ΔF/F0 images (top) and fluorescence time courses (bottom) at different triads (colored arrow heads). (**f**) Spark frequency ($n = 5$ mice for each condition, 3–4 fibers per muscle). Data are mean ± SEM (*$P < 0.05$, WT vs. *mdx*, vehicle treated *mdx* vs. *mdx* plus S107). (**g**) Effect of oral S107 on *mdx* mice voluntary exercise. $N = 5$ animals for each condition, * $P < 0.05$. (**h**) Force frequency relationship in EDL muscle stimulated from 1 to 120 Hz (300 ms pulse trains, orange circles are S107 treated *mdx* mice, black squares are vehicle treated *mdx* mice, $n = 5$ for each, $P < 0.001$ using a two Way Analysis of Variance comparing S107 treated vs. vehicle treated *mdx* mice). (**i**) Effect of S107 on fatigue resistance using endurance protocol (30 Hz 300 ms trains every second for 300 s). Orange circles are S107 treated *mdx* mice, black squares are vehicle treated *mdx* mice, $n = 5$ for each, $P < 0.001$ using a two Way Analysis of Variance comparing S107 treated vs. vehicle treated *mdx* mice.